Cell-Level Pharmacokinetic Model of Granulocyte Colony-Stimulating Factor: Implications for Ligand Lifetime and Potency in Vivo

CASIM A. SARKAR[1] and DOUGLAS A. LAUFFENBURGER

Department of Chemical Engineering (C.A.S., D.A.L.), Biotechnology Process Engineering Center (C.A.S., D.A.L.), Department of Biology (D.A.L.), and Biological Engineering Division (D.A.L.), Massachusetts Institute of Technology, Cambridge, Massachusetts

This article is available online at http://molpharm.aspetjournals.org

ABSTRACT

The cytokine granulocyte colony-stimulating factor (GCSF) is of great clinical importance, with primary application to rapidly elevate the peripheral neutrophil levels of chemotherapy patients through accelerated granulopoiesis. However, these mature bloodstream neutrophils express the GCSF receptor (GCSFR), presenting a significant and specific clearance mechanism of circulating GCSF that increases with time. Here, we formulate a mathematical model that describes these cell-level GCSF/GCSFR dynamics and correlate the effect of these endocytic trafficking processes to ligand depletion in an in vitro culture. We further incorporate this cell-level model into an existing pharmacokinetic/pharmacodynamic (PK/PD) model, to gain insight into the effects that specific molecular and cellular parameters may have on overall PK/PD effects in vivo. Our cell-level model suggests that ligand depletion may be reduced in vitro by decreasing the endosomal affinity of endocytosed GCSF/GCSFR complexes, matching experimental findings. Additionally, our modified PK/PD model suggests that a GCSF analog with a modification that effectively eliminates renal clearance should have a significantly longer half-life in vivo and should therefore improve peripheral neutrophil counts. This is consistent with clinical studies on a polyethylene glycol chemical conjugate of GCSF termed SD/01. The model predicts that a GCSF analog that eliminates renal clearance and has reduced endosomal binding affinity may result in an even longer ligand half-life and increased neutrophil counts at a lower dose than either wild-type GCSF or SD/01. More generally, this type of hierarchical model provides a correlation between the molecular and pharmacological properties of a drug and may elucidate design goals for such protein therapeutics.

Currently, the design and development of a therapeutic drug takes, on the average, 12 years and costs more than $800 million. Of this total cost, approximately one third is spent on drugs and experiments that fail. In addition, once a candidate drug makes it into clinical trials, the success rate is still less than 20%. One of the major problems in the development of a successful drug is the inability to correlate the effects of a molecular perturbation in the drug to the resulting effects in efficacy and half-life in vivo. This correlation can be particularly nonintuitive for protein therapeutics, such as hematopoietic cytokines, that act as agonists for cell-surface receptors.

The pharmacodynamic properties of such agonists depend not only on receptor binding affinity but also on subsequent intracellular signaling cascades and endocytic trafficking of the cell-surface cytokine/receptor complexes. Endocytic trafficking often serves to attenuate the generated signals, resulting in ligand depletion and receptor down-regulation, which in turn reduces the pharmacodynamic potency of the drug over time. Furthermore, the pharmacokinetic profile of such a cytokine is often determined not only by nonspecific renal and hepatic clearance mechanisms but also through specific endocytosis and degradation by local and systemic cell populations expressing the target receptor (Layton et al., 1989). Thus, optimization of cell-surface binding and endocytic trafficking properties could improve both the pharmacodynamic and pharmacokinetic properties of the drug. An understanding of the molecular properties that govern cytokine/receptor dynamics in the context of these cellular processes may help to optimize the design of the therapeutic protein.

An important instance in which altered trafficking of the ligand may have a significant impact on these in vivo properties is the cytokine granulocyte colony-stimulating factor (GCSF). GCSF is indicated for a wide range of clinical applications, primarily for cancer patients undergoing chemother-

ABBREVIATIONS: GCSF, granulocyte colony-stimulating factor; GCSFR, granulocyte colony-stimulating factor receptor; PK, pharmacokinetic; PD, pharmacodynamic; ANC, absolute neutrophil count; PEG, polyethylene glycol.

apy and other neutropenic patients (Morstyn et al., 1998). The drug is typically administered subcutaneously or intravenously; once it has entered the bloodstream, it diffuses into the bone marrow, where it binds to its receptor (GCSFR) on precursor cells, inducing them to proliferate and differentiate into mature neutrophils. These mature neutrophils then enter the bloodstream. In this manner, the cytokine rapidly elevates peripheral neutrophil counts in these immunocompromised patients so that they are less susceptible to serious complications from infection. However, the bone marrow precursor cells internalize and degrade the ligand—a negative feedback mechanism that can reduce its pharmacodynamic potency. Additionally, the mature neutrophils also express GCSFR, and they bind, internalize, and degrade the drug from the bloodstream. Thus, given the large number of these neutrophils, there exists a substantial second negative feedback loop that operates through much larger space in vivo and reduces the lifetime of the drug.

Herein, we report the development of a mathematical model that relates extracellular ligand depletion to the molecular properties of GCSF and cells expressing the GCSF receptor. We have further integrated this cell-level model to a physiologically relevant pharmacokinetic/pharmacodynamic (PK/PD) model. Currently, there is little mechanistic understanding as to how the various levels of biological complexity—from molecular interactions to cellular function to tissue organization and beyond—are integrated. The hierarchical model described here attempts to tie together these various biological levels and, for the specific case of GCSF, the model provides some insight into the molecular parameters of the therapeutic protein that should be varied to improve clinical efficacy.

Materials and Methods

Our cell-level mathematical model describes the fate of extracellular ligand and cell receptors over time. These molecules form complexes at the cell surface, become internalized into endosomal compartments, and undergo sorting to either recycling or degradation (Fig. 1). The model variables, parameters, and equations that describe these processes are given in Tables 1 and 2 and Fig. 2, respectively. Although it does not treat every step explicitly, this model attempts to capture the salient features of ligand/receptor trafficking dynamics that may have predictive value.

The cell-level model simulates the time-progression of the following variables: extracellular ligand concentration (L), free surface receptors per cell (R_s), surface complexes per cell (C_s), intracellular ligand concentration per cell (L_i), free intracellular receptors per cell (R_i), intracellular complexes per cell (C_i), and degraded ligand per cell (L_d) over the course of several days during which the cell density (N) is increasing. We can then use this kinetic model to simulate ligand depletion and endosomal sorting after an initial bolus of ligand into the extracellular medium, and compare these with experimental results that were obtained using a GCSF-dependent cell line, OCI/AML1. In the absence of ligand ($L = 0$), the variables C_s, L_i, C_i, and L_d are also zero, because each of these species requires ligand to be present. Furthermore, because we are simulating ligand-dependent cell growth, N is time-invariant in the absence of any initial ligand. Under these conditions, as is clear from eq. 1 in Fig. 2, the number of steady-state surface receptors per cell ($R_{s,ss}$) is determined from a balance between constitutive receptor endocytosis (k_{eR}) and receptor synthesis (V_s); specifically, $R_{s,ss} = V_s/k_{eR}$. Likewise, from eq. 4, the number of steady-state intracellular receptors per cell ($R_{i,ss}$) is set by the degradation rate constant (k_{deg}) and the receptor synthesis rate (V_s); specifically, $R_{i,ss} = k_{eR} \times R_{s,ss}/k_{deg} = V_s/k_{deg}$. These values serve as initial conditions for the cell-surface and intracellular receptors in simulations performed with nonzero initial extracellular ligand.

An extracellular ligand molecule can bind reversibly to a surface receptor (with the forward rate constant, k_f, linked to the reverse rate constant, k_r, through the equilibrium dissociation constant, $K_D = k_r/k_f$). These surface complexes are then internalized (k_{eC}) into endosomal compartments, which have a volume V_e per cell. Under these intracellular conditions, the ligand/receptor dynamic can be significantly different (k_{fi}, k_{ri}, and $K_{Di} = k_{ri}/k_{fi}$); therefore, intracellular receptor occupancy may also vary from that seen on the cell surface. From the endosomes, the molecules are either recycled intact back to the cell membrane and extracellular medium or degraded in lysosomal compartments. There is evidence that GCSF receptors and similar cytokine receptors are degraded upon internalization (Khwaja et al., 1993), and intracellular complexes and intracellular receptors are therefore routed to degradation (k_{deg}). Conversely, we allow ligand molecules that dissociate from intracellular receptors to recycle back out of the cell intact (k_{rec}).

Thus, in tracking the ligand molecules throughout these cellular processes, there is a ligand molecule associated with L, L_i, L_d, C_s, and C_i. As a consistency check, a mass balance on the five equations for
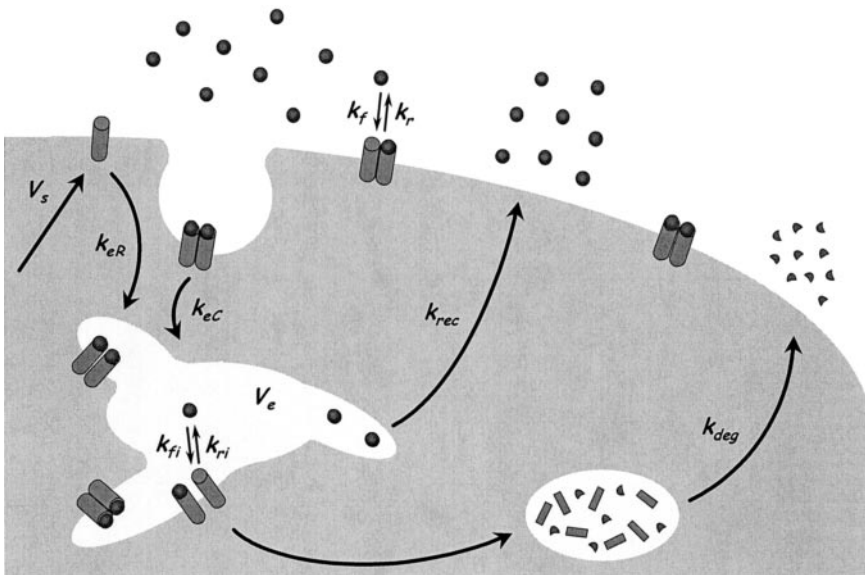

Fig. 1. Cell-level trafficking model for the GCSF/GCSFR system. Model parameters are defined in Table 2, and the corresponding equations are given in Fig. 2.

TABLE 1
Model variables

	Description
Cell-level model variables	
N	Cell density, number/liter
R_s	Cell-surface receptors, number/cell
C_s	Cell-surface complexes, number/cell
L_i	Intracellular ligand, M
R_i	Intracellular receptors, number/cell
C_i	Intracellular complexes, number/cell
L	Extracellular ligand (or main compartment ligand), M
L_d	Degraded ligand, number/cell
Additional PK/PD model variables	
L_4	Ligand in second compartment, M
n_1	Bisegmental absorption site 1 from subcutaneous dose, moles
n_2	Bisegmental absorption site 2 from subcutaneous dose, moles

these species reveals that the total ligand in the system (intact + degraded) is indeed conserved:

$$\frac{dL_{total}}{dt} = \frac{d\left(L + NL_iV_e + (C_s + C_i + L_d) \cdot \frac{N}{N_A} \right)}{dt} = 0 \quad (11)$$

The intention in developing this model was to see whether it could capture the gross features seen experimentally, both in ligand depletion and endosomal sorting studies. Our previous experimental results showed differential depletion and sorting properties for wild-type GCSF and two single Asp→His mutants, D110H and D113H (Sarkar et al., 2002). The two mutants were found to bind the cell-surface receptor with the same affinity as wild type and they also internalized at the same rate. However, the mutants bound with lower affinity to the receptor than wild type at endosomal pH, resulting in enhanced ligand recycling and ligand half-life.

The parameters for the cell-level model were either measured experimentally or taken from the literature. Although the actual values were obtained from heterogeneous cell types, the trends observed from model simulations are largely insensitive to a change in any particular constant that is less than an order of magnitude. The receptor synthesis rate was chosen so that the steady-state number of surface receptors (5000) would be comparable with values reported in the literature (Elsonbaty et al., 1995a,b; Morikawa et al., 1996). The equilibrium endosomal affinity for wild-type GCSF was the only fitted parameter in the model. The affinity of wild-type GCSF was 1.7-fold lower when measured at pH 5.5 rather than at pH 7.4 (Sarkar et al., 2002); however, the pH difference alone does not necessarily provide a true indication of the endosomal environment. Therefore, the experimental value (1.7) was multiplied by a factor of 50 to account for these potential environmental differences ($K_{Di} = 85$ K_D for wild type). The experimentally measured endosomal affinities of the mutants (4.4-fold lower for D110H and 6.8-fold lower for D113H) were also multiplied by this same scaling factor for the model ($K_{Di} = 220$ K_D for D110H and $K_{Di} = 340$ K_D for D113H). Although it would be possible to use a different value for the scaling factor to fit the experimental results for each histidine mutant, this would provide no validation in correlating the endosomal affinities to the ligand sorting and depletion results. Therefore, the scaling factor was held constant for all simulations (although the experimentally measured endosomal affinities were different for each ligand) and the ability of the model to accurately predict the endosomal sorting and ligand depletion profiles of the mutants was tested. The model does not directly account for a sorting time of 5 to 10 min before recycling or degradation (Lauffenburger and Linderman, 1993); during this time, internalized complexes are allowed to dissociate and possibly reassociate—the endosomal affinity is typically weaker, and the dissociation rate constant larger—before these resulting intracellular species are shuttled to either recycling or degradation. In particular, the only effect of this sorting time on our model is the generation of free ligand for recycling (with free receptors and remaining complexes being degraded) and, for GCSF/GCSFR, this reversible endosomal interaction is predicted to reach equilibrium within this sorting time for a 2-fold faster dissociation rate constant. Therefore, for the sake of simplicity in formulation of the model, we

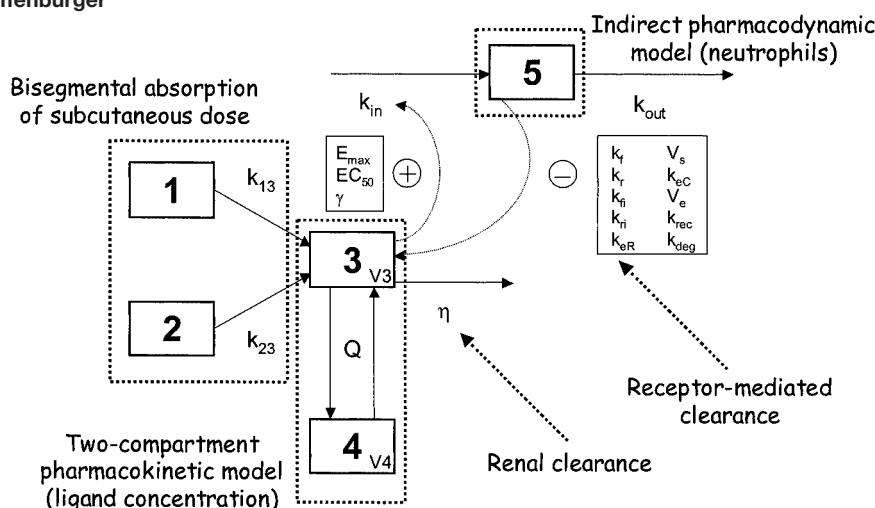| Cell-level model		PK/PD model	
$\frac{d(NR_s)}{dt} = \left(- k_f L R_s + k_r C_s - k_{eR} R_s + V_s\right) \cdot N$			[1]
$\frac{d(NC_s)}{dt} = \left(k_f L R_s - k_r C_s - k_{eC} C_s\right) \cdot N$			[2]
$\frac{d(NL_i)}{dt} = \left(\left(- k_{fi} L_i R_i + k_{ri} C_i\right) \cdot \frac{1}{N_A V_e} - k_{rec} L_i\right) \cdot N$			[3]
$\frac{d(NR_i)}{dt} = \left(- k_{fi} L_i R_i + k_{ri} C_i + k_{eR} R_s - k_{deg} R_i\right) \cdot N$			[4]
$\frac{d(NC_i)}{dt} = \left(k_{fi} L_i R_i - k_{ri} C_i + k_{eC} C_s - k_{deg} C_i\right) \cdot N$			[5]
$\frac{dL}{dt} = \left(- k_f L R_s + k_r C_s + k_{recL} L_i V_e N_A\right) \cdot \frac{N}{N_A} - k_{1,WT} L$	[6']	$\frac{dL}{dt} = \frac{1}{V_3} \cdot \left(k_{13} n_1 + k_{23} n_2 - \eta L + Q \cdot (L_4 - L)\right)$ $+ \left(- k_f L R_s + k_r C_s + k_{rec} L_i V_e N_A\right) \cdot \frac{N}{N_A}$	[6]
$\frac{d(NL_d)}{dt} = \left(k_{deg} C_i\right) \cdot N$	[7']		
		$\frac{dL_4}{dt} = \frac{Q}{V_4} \cdot (L - L_4)$	[7]
		$\frac{dN}{dt} = k_{in} \cdot \left(1 + \frac{E_{max} \left(\frac{L K_{D,WT}}{K_D}\right)^{\gamma}}{EC_{50}{}^{\gamma} + \left(\frac{L K_{D,WT}}{K_D}\right)^{\gamma}}\right) - k_{out} N$	[8]
		$\frac{dn_1}{dt} = -k_{13} n_1$	[9]
		$\frac{dn_2}{dt} = -k_{23} n_2$	[10]

Fig. 2. Model equations.

Fig. 3. Modified PK/PD model incorporating cell-level model. 1 and 2, bisegmental absorption sites; 3, main ligand compartment; 4, secondary ligand compartment; 5, absolute neutrophil counts. Neutrophil production is indirectly stimulated by the amount of ligand in compartment 3; depletion of ligand in compartment 3 is accelerated by neutrophils through receptor-mediated uptake and degradation (as implemented by the cell-level model, Fig. 1). The corresponding equations are given in Fig. 2.

accelerate the endosomal kinetics 100-fold to allow this equilibrium to take place rapidly relative to the transport rates associated with the subsequent sorting steps. This avoids the need to incorporate a lag time into the model and allows for continuous, rather than batch, processing of complexes entering endosomal compartments in our whole-cell kinetic model. Because wild-type GCSF is prone to aggregation at neutral pH, an additional term was included that accounts for this loss ($k_{l,WT}$) over time. This rate constant was determined from experimental measurements in which approximately 75% of GCSF remained intact after 6 days in culture with a YT-2C2 cell line that does not express GCSFR.

Model simulations were run on MATLAB using the *ode15s* subroutine. Ligand depletion was simulated over a period of 8 days with an initial ligand concentration of 125 pM, the same conditions as in experiments. Cell density was expressed as an exponential function that matched experimental data with an initial density of 10^8 cells/liter. For endosomal sorting simulations, cells were exposed to a bolus of extracellular ligand for 180 min, after which time the values for R_s, R_i, C_i, and L_i were recorded. These values were then used as initial conditions in a second simulation, in which the initial ligand concentration and k_f were set to zero; k_f was set to zero to prevent recycled ligand from rebinding to cell-surface receptors. Then, the values for L (intact) and L_d (degraded) were recorded for 15 min. The computational sorting fraction was then calculated from the average of three time points (5, 10, and 15 min), as was done experimentally. This procedure was performed for wild-type GCSF and both mutants, with the mutants having reduced endosomal binding affinities, as described above.

The full PK/PD model is shown schematically in Fig. 3 and can be described by the more complete set of equations in Fig. 2, which are adapted from the model by Wang et al. (2001) to incorporate the cell-level model. The intent here is not to fully reproduce the original PK/PD model proposed by Wang et al. (2001), but to take the salient features of that model and combine them with the cell-level model to generate a modified PK/PD model that explicitly includes molecular and cellular parameters.

In the original PK/PD model, two different doses of GCSF (750 and 375 μg) were administered subcutaneously to patients to generate experimental data for fitting their model parameters (Wang et al., 2001). The dosing was best fit by a bisegmental absorption model, treating the fractional bioavailability of the total dose as two theoretically separate dose sites (n_1 and n_2). These doses then enter the bloodstream (main compartment concentration, L), where they can be cleared by renal, hepatic, and other nonspecific clearance mechanisms (lumped parameter, η). In the original model, a saturable

clearance mechanism was also included, but because this is likely to represent the receptor-mediated clearance by peripheral neutrophils, this implicit mechanism was replaced by the explicit cell-level model. The data are best fit by a two-compartment model, and the concentration of the drug in the second compartment (L_4) is driven by the interchange (Q, same value in both directions) between the two compartments. This second compartment does not necessarily correspond to some organ or actual location in the body; rather, it serves as a computational means for more precisely mimicking drug pharmacokinetic profiles, and the flow rate, Q, between these two compartments is a fitted parameter in the model. Finally, in the original PK/PD model, the concentration of drug in the main compartment indirectly augments neutrophil production above basal levels (k_{in}) through a saturable mechanism (E_{max}, EC$_{50}$) with cooperativity, γ (Wang et al., 2001):

$$production = k_{in} \cdot \left(1 + \frac{E_{max}L^\gamma}{EC_{50}^\gamma + L^\gamma} \right) \qquad (12)$$

The cooperativity, γ, is another fitted parameter in the model that has no direct biological interpretation; rather, it is a measure of the sensitivity of neutrophil production to drug concentration (the larger the cooperativity, the greater the sensitivity). Although this production effect is expressed as a function of absolute drug concentration (L), it is probably more important to consider the number of complexes that the drug can form on the surface of bone marrow precursor cells (as an initial approximation), because the complexes generate the signals to proliferate and differentiate into mature neutrophils (Fallon and Lauffenburger, 2000). In other words, if we designed an analog of the drug that had lower binding affinity for the receptor, it could reduce receptor-mediated clearance in the bloodstream, but it might also have reduced potency in generating such signals on the time scale of interest. A more relevant value to consider is L/K_D, and we have therefore substituted ($L \times K_{D,WT}/K_D$) for L in describing neutrophil production (see Fig. 2).

Results

Comparison of Cell-Level (in Vitro) Model Predictions with Experimental Results

The cell-level model is intended to simulate endosomal sorting and extracellular depletion of ligand. Previously, we determined the endosomal sorting fraction of wild-type GCSF experimentally using a GCSF-dependent human sus-

TABLE 2
Model parameters

Parameters	Base Value	Description
Cell-level model		
K_D	150×10^{-12} M	Extracellular equilibrium dissociation constant (C. A. Sarkar, K. Lowenhaupt, P. J. Wang, T. Horan, and D. A. Lauffenburger, unpublished observations)
k_r	0.03/min	Extracellular dissociation rate constant (Sarkar, 2002)
k_f	k_r/K_D	Extracellular association rate constant
K_{Di}	$85\,K_D$	Intracellular equilibrium dissociation constant, see *Materials and Methods*
k_{ri}	$100\,k_r$	Intracellular dissociation rate constant, see *Materials and Methods*
k_{fi}	k_{ri}/K_{Di}	Intracellular association rate constant
k_{eR}	0.005/min	Constitutive receptor endocytosis rate constant (Kuwabara et al., 1996)
V_s	25/min	Receptor synthesis rate, see *Materials and Methods*
k_{eC}	0.10/min	Complex endocytosis rate constant (Sarkar et al., 2002)
V_e	10^{-14} liters	Endosomal volume (French et al., 1995)
N_A	6.02×10^{23} molecules/mole	Avogadro's number
k_{rec}	0.15/min	Recycling rate constant (Ghosh et al., 1994)
k_{deg}	0.059/min	Degradation rate constant (Kuwabara et al., 1996)
$k_{l,WT}$	4.17×10^{-5}/min	Rate constant for loss of functional wild type from medium (C. A. Sarkar, and D. A. Lauffenburger, unpublished observations)
Additional PK/PD model[a]		
V_3	1.81 liters	Volume of main compartment
k_{13}	0.0044/min	Absorption rate constant from site 1 to main compartment
k_{23}	0.0033/min	Absorption rate constant from site 2 to main compartment
η	0.0049 liter/min	Rate constant for nonspecific clearance of L
Q	4.65×10^{-4} liter/min	Rate of interchange between main and secondary compartments
V_4	0.249	Volume of secondary compartment
k_{in}	3.13×10^6 cells/liter/min	Basal neutrophil production rate
E_{max}	12.7	Maximal fold increase in basal neutrophil production rate
EC_{50}	2.53×10^{-10} M	Wild-type concentration eliciting half-maximal increase in basal neutrophil production rate
γ	1.34	Hill coefficient
k_{out}	7.57×10^{-4}/min	Neutrophil decay rate constant

[a] Values from Wang et al. (2001).

pension cell line, OCI/AML1 (Sarkar et al., 2002). We have also used this cell line to quantify the extracellular depletion of wild type over a time course of 8 days, during which the cell density was increasing. We have also measured the endosomal sorting fractions and ligand depletion profiles for two single mutants of GCSF, D110H and D113H (Sarkar et al., 2002). These analogs were rationally designed to maintain similar trafficking properties to wild-type GCSF, except that the histidine residues would contribute to lower affinity binding at endosomal pH. This, in turn, was predicted to enhance endosomal sorting to recycling and therefore decrease extracellular ligand depletion.

Wild-type experiments were simulated using the base parameter values given in Table 2. The trials for the histidine mutants were performed identically, except that the endosomal affinity (K_{Di}) was proportionally changed to match experimental measurements ($K_{Di} = 220\,K_D$ for D110H and $K_{Di} = 340\,K_D$ for D113H). For endosomal sorting simulations, cells were exposed to a bolus of extracellular ligand for 180 min, after which time the values for R_s, R_i, C_i, and L_i were recorded. These values were then used as initial conditions in a second simulation, in which the initial ligand concentration and k_f were set to zero; k_f was set to zero to prevent recycled ligand from rebinding to cell-surface receptors (again to match the experimental conditions in which the surface receptors were blocked before measuring intact and degraded ligand). Then, the values for L (intact) and L_d (degraded) were recorded for 15 min. The computational sorting fraction was then calculated from the average of three time points (5, 10, and 15 min), as was done experimentally. The computational endosomal sorting fraction was insensitive to the initial bolus of extracellular ligand. This procedure was per-

formed for wild-type GCSF and both mutants, with the mutants having reduced endosomal binding affinities, as described above. For the experiments and simulations of each analog, the average and S.D. of these three time points are reported in Table 3.

The ligand depletion experiments were simulated over 8 days with an initial cell density of 10^8/liter and an initial extracellular ligand concentration of 125 pM to match the experimental conditions. Because the cell line used is GCSF-dependent, exponential growth (specific growth rate, 0.277/day) was included to account for changing cell density, $N(t)$. The fraction of intact ligand in the extracellular medium after this time period is reported in Table 3.

The results in Table 3 indicate that the model, even with lumped parameters from heterogeneous sources, can effectively capture the cellular trafficking dynamics observed experimentally. We have therefore integrated this cell-level model into an existing PK/PD model to understand how the parameters in this full model might impact the efficacy of the drug in an in vivo setting. The remaining results focus on observations from this modified PK/PD model, with results showing the sensitivities of $L(t)$ and $N(t)$ to changes in model parameters.

TABLE 3
Comparison of cell-based experiments and cell-level model

	Ligand Sorting Fraction		Fraction of Ligand Intact after 8 Days	
	Experiment	Model	Experiment	Model
Wild Type	0.44 ± 0.08	0.45 ± 0.04	0.04 ± 0.00	0.20 ± 0.03
D110H	0.66 ± 0.02	0.63 ± 0.03	0.78 ± 0.01	0.59 ± 0.03
D113H	0.62 ± 0.02	0.70 ± 0.04	0.76 ± 0.02	0.67 ± 0.06

In Vivo Predictions on Ligand Depletion and Neutrophil Counts from Modified PK/PD Model

The modified PK/PD model, in which we have omitted the saturable clearance mechanism and integrated the cell-level model (Fig. 3), suggests that neutrophil production—the desired result from GCSF therapy—is correlated to the concentration of ligand in the bloodstream (compartment 3). Therefore, mechanisms that deplete the ligand would reduce neutrophil production. To understand the extent to which the parameters in the model affect ligand depletion and neutrophil counts, we have monitored these two variables in response to the sensitivities of certain model parameters. In most cases, the sensitivities were simulated with two different amounts of subcutaneously injected ligand (375 or 750 μg). The absolute neutrophil count (ANC) at the beginning of

the simulation was fixed by the basal rate of production (k_{in}) and the rate of decay (k_{out}).

Effects of Nonspecific Clearance (η). Most therapeutics are administered at levels that are far above the concentrations needed to elicit the appropriate response in vivo. Often, this has to be done because of rapid nonspecific clearance mechanisms in the body that make it difficult to sustain the physiologically normal levels over extended periods of time. In the case of wild-type GCSF, primarily renal clearance limits the half-life of the drug to several hours, whereas the time course of therapy is often several days (Morstyn et al., 1998). Therefore, treatment necessitates multiple, artificially high doses of GCSF to the patient. Because these nonspecific clearance mechanisms can depend significantly on molecular dimensions, artificially increasing the size of
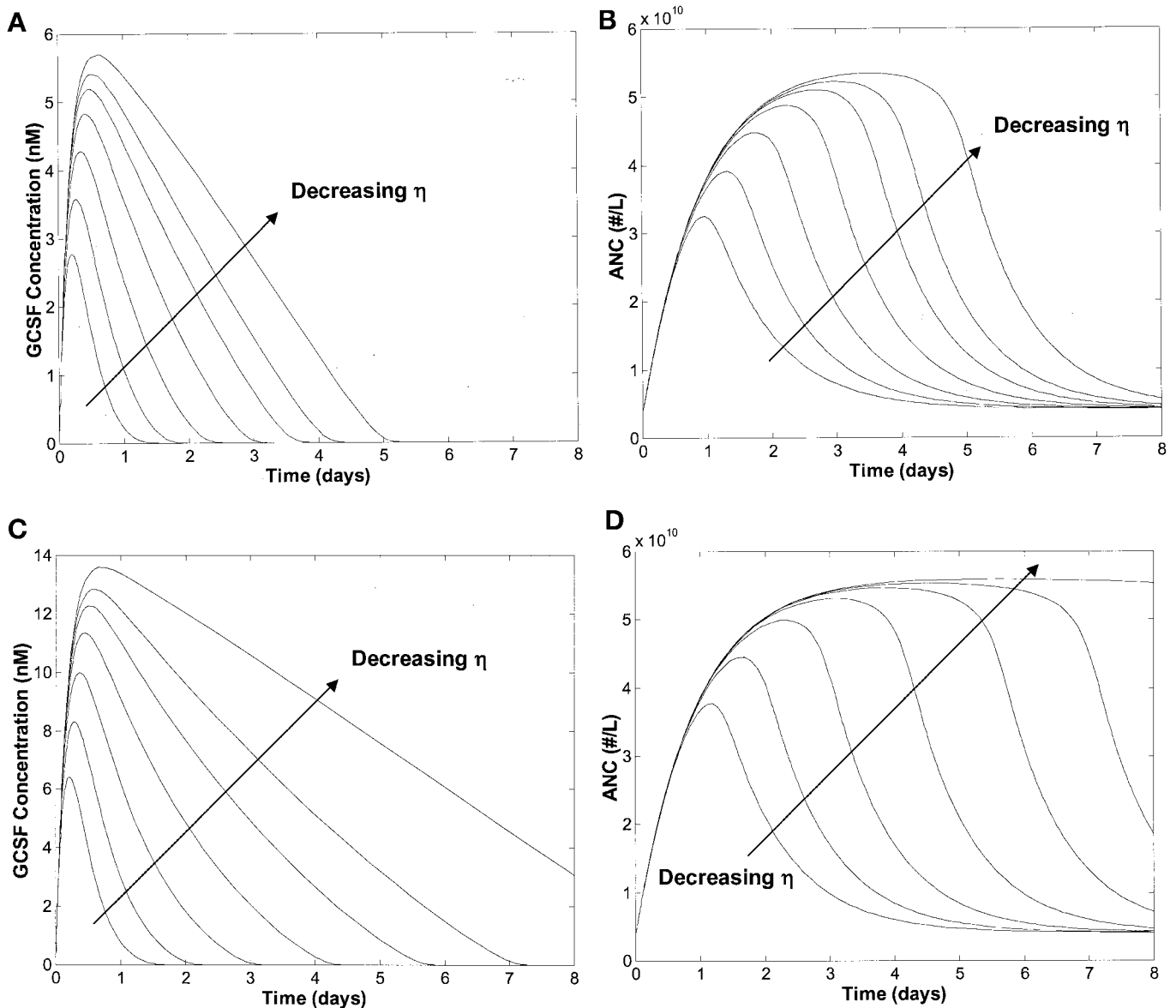

Fig. 4. Sensitivities of GCSF concentration and ANC to nonspecific clearance, η, after initial subcutaneous injection. A, sensitivity of GCSF concentration with 375-μg dose, $\eta = 0.0049 \times (1, 1/2, 1/4, 1/8, 1/16, 1/32, 0)$ L/min. B, sensitivity of ANC with 375-μg dose, $\eta = 0.0049 \times (1, 1/2, 1/4, 1/8, 1/16, 1/32, 0)$ L/min. C, sensitivity of GCSF concentration with 750-μg dose, $\eta = 0.0049 \times (1, 1/2, 1/4, 1/8, 1/16, 1/32, 0)$ L/min. D, sensitivity of ANC with 750-μg dose, $\eta = 0.0049 \times (1, 1/2, 1/4, 1/8, 1/16, 1/32, 0)$ L/min.
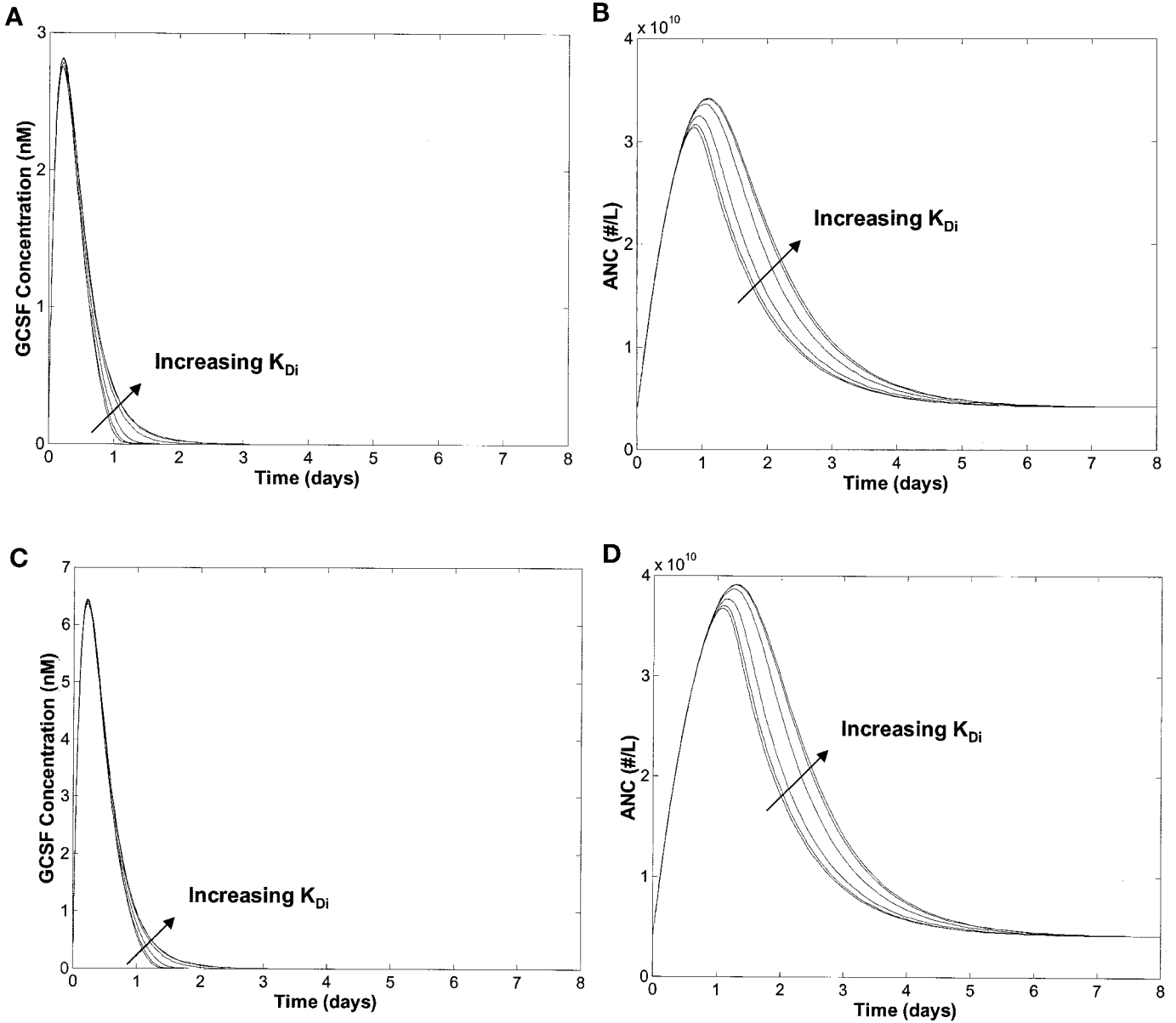
A

B

C

D

Fig. 5. Sensitivities of GCSF concentration and ANC to endosomal binding affinity, K_{Di}, after initial subcutaneous injection. A, sensitivity of GCSF concentration with 375-μg dose, $K_{Di} = 85\ K_D \times (0.01, 0.1, 1, 10, 100, \infty)$. B, sensitivity of ANC with 375-μg dose, $K_{Di} = 85\ K_D \times (0.01, 0.1, 1, 10, 100, \infty)$. C, sensitivity of GCSF concentration with 750-μg dose, $K_{Di} = 85\ K_D \times (0.01, 0.1, 1, 10, 100, \infty)$. D, sensitivity of ANC with 750-μg dose, $K_{Di} = 85\ K_D \times (0.01, 0.1, 1, 10, 100, \infty)$.

the molecule may help to reduce these clearance mechanisms. This can often be achieved by covalently attaching a bulky, inert moiety to the drug. Typically, polyethylene glycol (PEG) is chosen because it is known to be bioinert and the chemistry can be controlled well (Delgado et al., 1992). This approach has shown promise in studies of many growth factors and cytokines, including interleukin-6, megakaryocyte growth and development factor, and interleukin-2 (Harris et al., 2001).

Recently, the Food and Drug Administration approved a PEG-conjugated GCSF molecule (termed SD/01) for therapeutic use. The PEG moiety is 20 kDa in size and is attached to the N terminus of GCSF, which alone is only approximately 19 kDa. The PEG modification effectively eliminates renal clearance of the drug (Johnston et al., 2000); therefore, depletion is essentially mediated by neutrophil uptake and

degradation. The experimentally measured lifetime of SD/01 is dose-dependent, but is approximately 4 to 5 days in rats (Morstyn et al., 2001).

We determined the effects of the nonspecific clearance on ligand concentration, L (from compartment 3), and the absolute neutrophil count, N. The parameter η was varied from the base value to zero, and the resulting ligand concentration and ANC profiles were recorded (Fig. 4). This figure shows increases in ligand half-life that correspond well with experimental observations with SD/01. Furthermore, the neutrophil counts achieve greater peak values and also maintain higher levels for longer periods of time as η is decreased.

Effects of Endosomal Binding Affinity (K_{Di}). Because it was clear from our in vitro studies and from the cell-level model that decreasing the endosomal binding affinity (K_{Di}) could improve the ligand sorting fraction and enhance ligand

half-life, we wanted to determine the effect of this parameter on ligand depletion and neutrophil counts in the PK/PD model. As seen in Fig. 5, there is a small increase in GCSF concentration as the endosomal affinity is decreased; however, this still expands the neutrophil profile by up to 1 day. This can be explained by the fact that the K_D for GCSF is approximately 150 pM, whereas the subcutaneous doses are resulting in ligand concentrations in the nanomolar range. Thus, the apparently small increase in intact ligand between days 1 and 2 is sufficient to elicit a significant improvement in neutrophil production. Given these artificially high doses, it is more desirable to have a small amount of ligand available for a long period of time than to have a large initial dose of ligand that is rapidly depleted.

Effects of Extracellular Binding Affinity (K_D) in the Absence of Nonspecific Clearance. Because it is possible to eliminate renal clearance of GCSF through PEG-modification (Johnston et al., 2000), we focus on the effects of specific cellular parameters on the modified PK/PD model in the absence of nonspecific clearance ($\eta = 0$). Under these conditions, the only mechanism by which ligand can be cleared in the model is through specific receptor-mediated endocytosis and degradation. One mechanism for reducing this depletion would be to decrease the flux of ligand molecules into the cell. This could be achieved in two ways: decreasing the internalization rate constant or decreasing the extracellular binding affinity. Because at present we do not know how to manipulate the ligand in a way that would decrease the internalization rate constant, we focus on the effect of extracellular binding affinity on ligand depletion and neutrophil enhancement. Although it is clear that decreasing the extracellular binding affinity should increase ligand half-
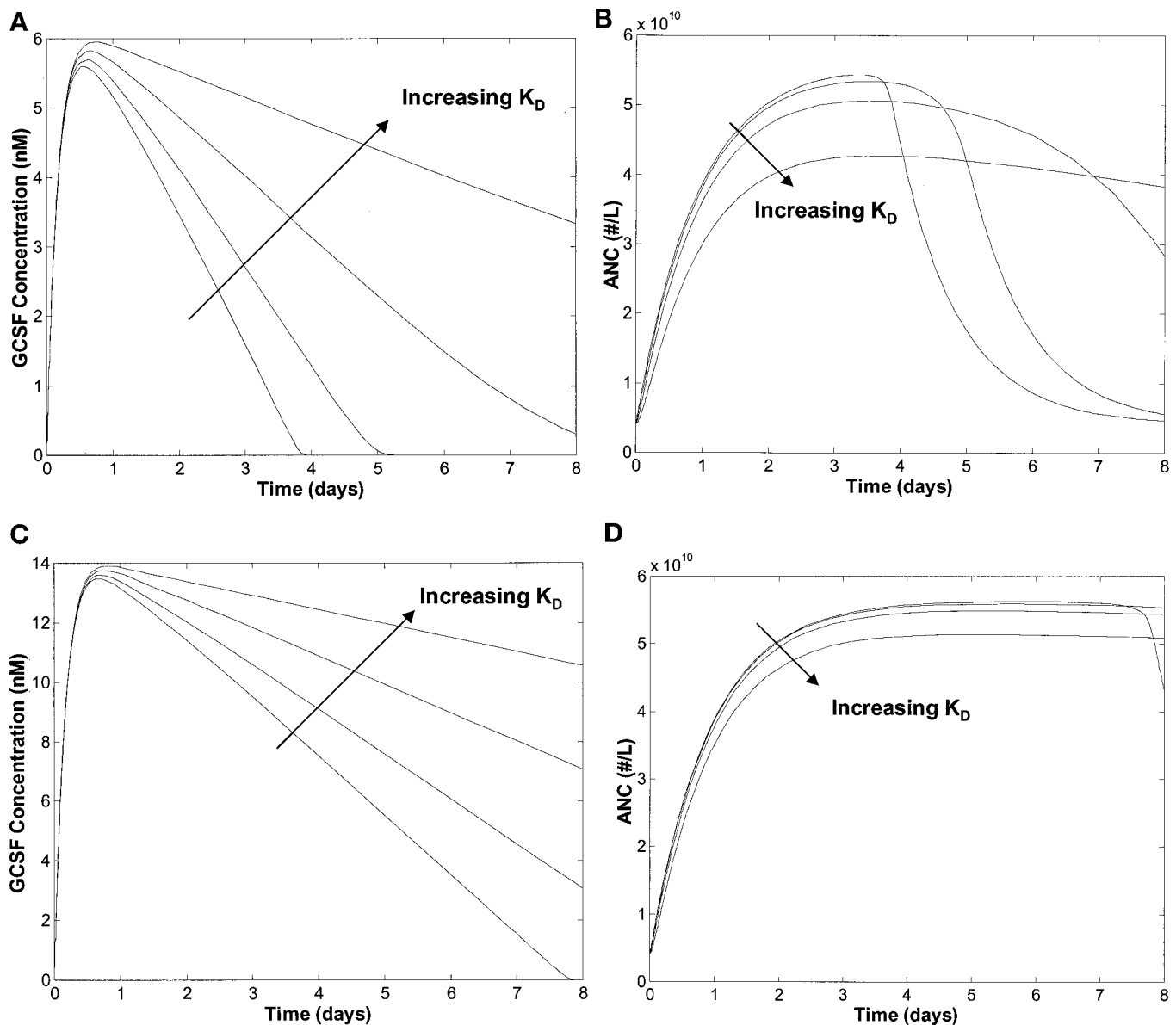

Fig. 6. Sensitivities of GCSF concentration and ANC to extracellular receptor binding affinity, K_D, in the absence of nonspecific clearance ($\eta = 0$) after initial subcutaneous injection. A, sensitivity of GCSF concentration with 375-μg dose, K_D = 50, 150, 450, 1350 pM. B, sensitivity of ANC with 375-μg dose, K_D = 50, 150, 450, 1350 pM. C, sensitivity of GCSF concentration with 750-μg dose, K_D = 50, 150, 450, 1350 pM. D, sensitivity of ANC with 750 μg-dose, K_D = 50, 150, 450, 1350 pM.
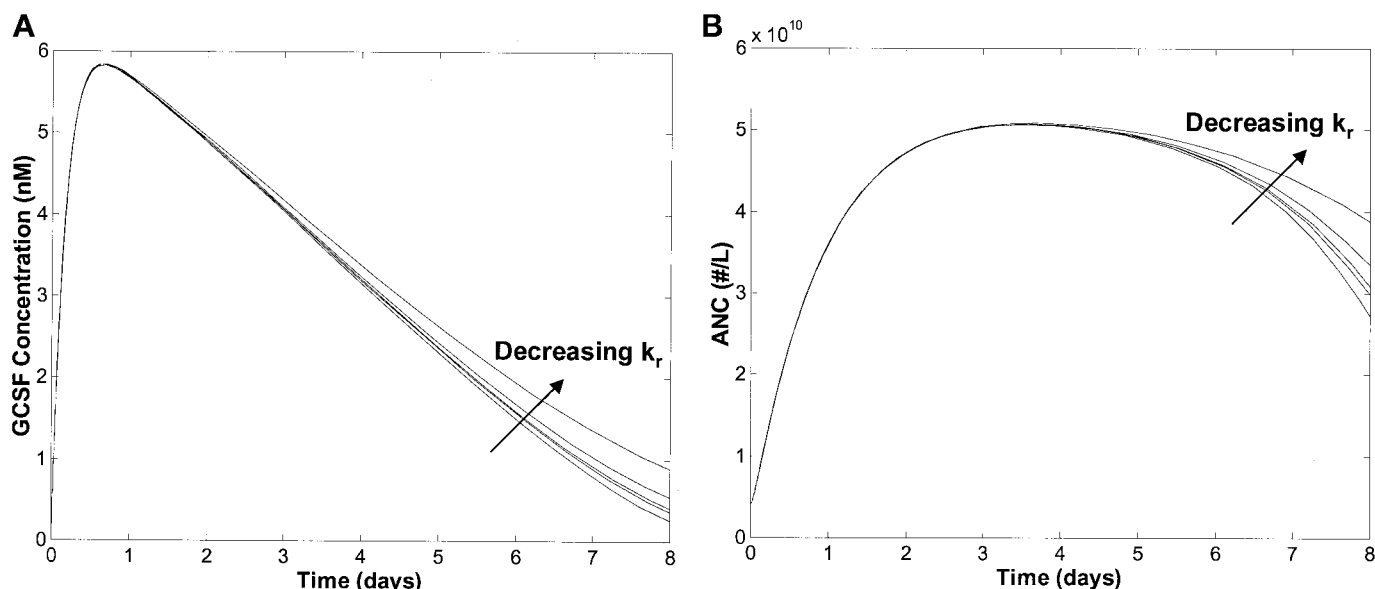
Fig. 7. Sensitivities of GCSF concentration and ANC to extracellular binding kinetics, k_r and k_f, in the absence of nonspecific clearance ($\eta = 0$) after initial subcutaneous injection of 375-μg dose. The K_D is held constant by varying both k_r and k_f by the same percentage. A, sensitivity of GCSF concentration, $k_r = 0.03 \times (1/10, 1/3, 1, 3, 10)$/min. B, sensitivity of ANC, $k_r = 0.03 \times (1/10, 1/3, 1, 3, 10)$/min.

life, eq. 8 in Fig. 2 suggests that this would also decrease the positive influence of ligand concentration on the neutrophil production rate. This tradeoff may explain why greatly increasing the binding affinity of a drug may not improve its efficacy and why greatly decreasing its affinity may also not result in improved efficacy; there is likely to be an optimal binding affinity for a particular therapeutic application.

Figure 6 shows the GCSF and neutrophil profiles for four hypothetical PEG-GCSF molecules ($K_D = 50, 150, 450, 1350$ pM). Although ligand depletion is not significant at the higher dose (Fig. 6, C and D), the neutrophil counts show some interesting behaviors at the lower dose (Fig. 6B). For the first 3 days, the neutrophil counts increase as the ligand binding affinity increases. However, the higher-affinity ligands are depleted more rapidly (Fig. 6A), which results in somewhat inverted neutrophil profiles at longer times. Although three of the curves maintain relatively similar neutrophil counts over the first 3 days ($K_D = 50, 150,$ and 450 pM), the 50 and 150 pM binders have rapidly decaying profiles, whereas the 450 pM binder maintains neutrophil counts at a high level over the entire time course. Thus, the ligand with the 450 pM equilibrium dissociation constant seems to be the best in this application.

Interestingly, although SD/01 was developed to eliminate renal clearance, we have shown that it does not maintain wild-type affinity to the receptor. We have measured the K_D of SD/01 to be about 450 pM (C. A. Sarkar, K. Lowenhaupt, P. J. Wang, T. Horan, and D. A. Lauffenberger, submitted for publication). This suggests that SD/01 may be optimized in multiple ways.

Effects of Extracellular Binding Kinetics in the Absence of Nonspecific Clearance. We further examined the effects of binding by simulating hypothetical variants of SD/01 with altered extracellular binding kinetics. None of these molecules had nonspecific clearance ($\eta = 0$), and they all had the same extracellular binding affinity ($K_D = 450$ pM). The kinetics for each hypothetical molecule were altered

by increasing or decreasing the extracellular association (k_f) and dissociation (k_r) rate constants by the same percentage, thus maintaining the equilibrium binding affinity. Figure 7 shows that the kinetics have a minimal effect on ligand concentration and neutrophil counts, although at long times, the neutrophil counts are slightly improved for lower k_r.

At short times, the ligand concentration is much greater than the K_D, and the system is therefore saturated. However, as the ligand concentration gets closer to the K_D, the kinetics of binding become more important and can change the efficacy of the drug. The results in Fig. 7 suggest that depletion is driven more by ligand association than by the lack of ligand dissociation, because ligand depletion is reduced for slower association. If depletion were driven more by the lack of ligand dissociation, then faster dissociation would save more ligand molecules from internalization. Thus, if GCSF were dosed at concentrations near the K_D, it could be more effective to administer an analog with slower binding kinetics.

Effects of Endosomal Binding Affinity (K_{Di}) in the Absence of Nonspecific Clearance. Although decreasing the extracellular binding affinity is a way to decrease ligand depletion (Fig. 6), there is a possible tradeoff of reduced pharmacodynamic potency because fewer signaling complexes are formed on the surface of the target cells in the timeframe of interest. This is manifested to a first approximation in eq. 8 in Fig. 2. However, an alternate way to decrease the amount of ligand depleted without altering surface binding properties is to route the internal ligand to recycling instead of degradation. We have shown that, for GCSF, the amount of ligand recycled (instead of degraded) can be enhanced by decreasing the endosomal affinity of the complex (Sarkar et al., 2002) and have captured this effect in our cell-level model (Table 3). This has also been shown for other ligand/receptor systems (French et al., 1995; Fallon et al., 2000), suggesting that this may be an important strategy for designing such ligands for therapeutic applications.
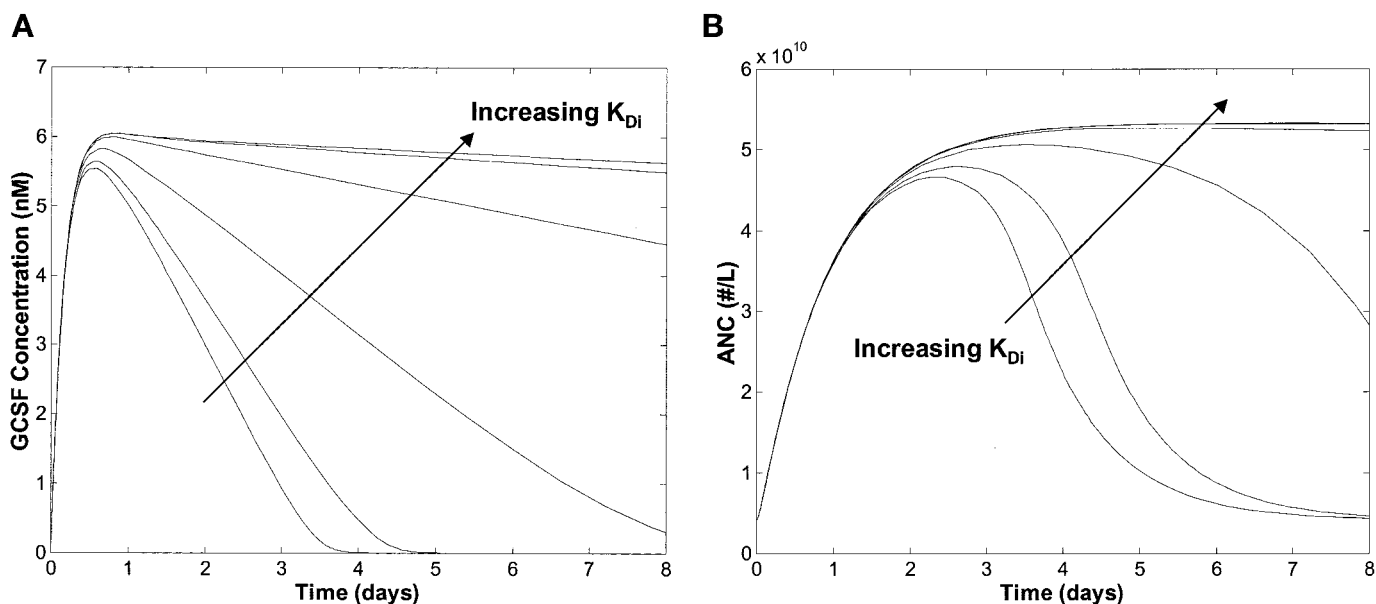
A

B

Fig. 8. Sensitivities of GCSF concentration and ANC to endosomal binding affinity, K_{Di}, in the absence of nonspecific clearance ($\eta = 0$) after initial subcutaneous injection of 375-μg dose. A, sensitivity of GCSF concentration, $K_{Di} = 85\ K_{D,SD/01} \times (0.01, 0.1, 1, 10, 100, \infty)$. B, sensitivity of ANC, $K_{Di} = 85\ K_{D,SD/01} \times (0.01, 0.1, 1, 10, 100, \infty)$.
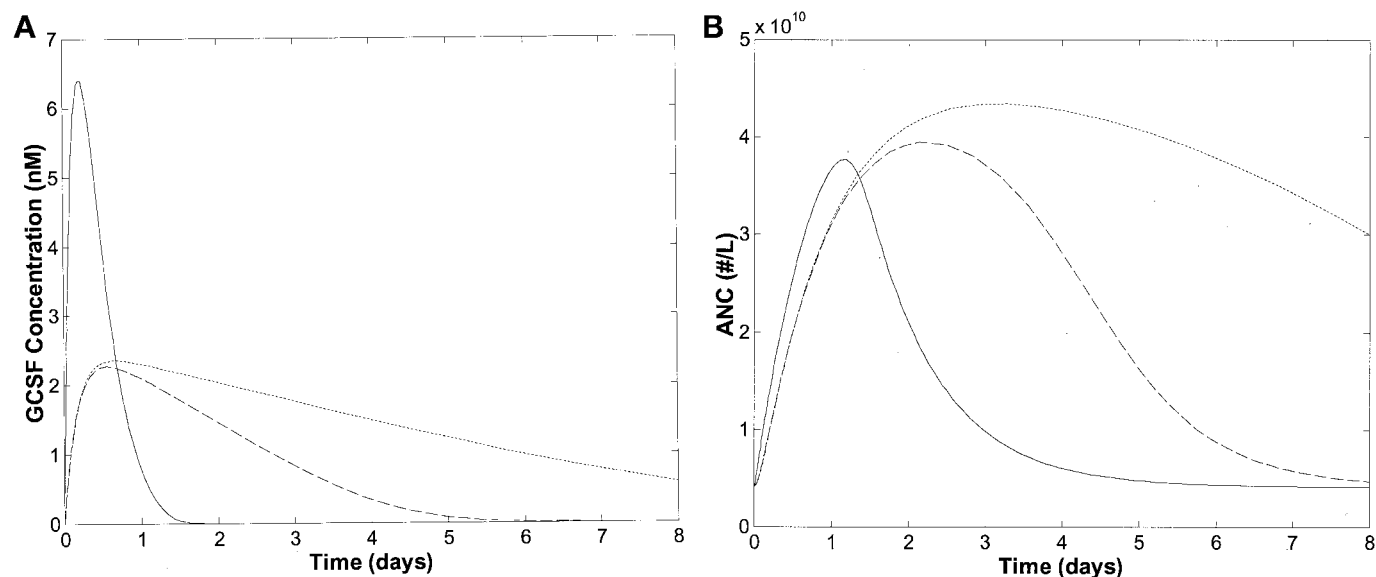
A

B

Fig. 9. Predicted concentration and ANC curves for wild type (750 μg, $n_{10} = 9.5 \times 10^{-9}$ mol and $n_{20} = 19.3 \times 10^{-9}$ mol; solid line), SD/01 (hypothetical dose, $n_{10} = 2.5 \times 10^{-9}$ mol and $n_{20} = 2.5 \times 10^{-9}$ mol; dashed line), and an SD/01-like molecule with 5-fold lower endosomal binding affinity ($K_{Di} = 5 \times 85\ K_{D,SD/01}$; hypothetical dose, $n_{10} = 2.5 \times 10^{-9}$ mol and $n_{20} = 2.5 \times 10^{-9}$ mol; dotted line). The hypothetical dose for each of the latter two molecules is about 17% of that for wild type in these simulations. A, concentration profiles for wild type (solid line), SD/01 (dashed line), and an SD/01-like molecule with 5-fold lower endosomal binding affinity (dotted line). B, ANC profiles for wild type (solid line), SD/01 (dashed line), and an SD/01-like molecule with 5-fold lower endosomal binding affinity (dotted line).

To determine the effects of endosomal binding affinity on ligand concentration and neutrophil counts in the PK/PD model, we simulated several theoretical SD/01-like molecules with reduced endosomal binding affinity. It is conceivable that this could be achieved in practice by adding a PEG-modification to one of the histidine mutants, D110H or D113H.

As seen in Fig. 8A, decreasing the endosomal affinity can greatly increase the ligand half-life. Furthermore, the effect

on neutrophil counts is even more dramatic (Fig. 8B). The neutrophil counts for the ligand with the highest endosomal affinity return to baseline after 8 days, whereas the counts for the ligand with the lowest endosomal affinity stay at the maximal value even at 8 days. A comparison of Figs. 6B and 8B shows that decreasing the extracellular binding affinity can reduce potency at short times, whereas that is not observed in the simulations in which only the endosomal binding affinity is decreased. Although this is a result of our

formulation of eq. 8 in Fig. 2, it is likely that this would be observed experimentally as well.

Comparison of Two Theoretical Doses of GCSF Analogs to Wild Type. In these simulations, we have observed that artificially high doses are required to sustain some level of therapeutic efficacy over a desirable time period. Often, even a single injection of such a large dose is insufficient for the entire treatment time, and multiple doses become necessary. The doses used in this work (375 and 750 μg, subcutaneous) were chosen from the PK/PD model formulated by Wang et al. (2001), because our model incorporates many of those model parameters, including the bioavailability and bisegmental absorption parameters for these two doses. Because the simulations indicate that an SD/01-like molecule and an SD/01-like analog with decreased endosomal binding affinity would have improved efficacy compared with wild-type GCSF, we tested whether they could be equally effective at lower doses. This would be beneficial to the patient, the supplier, and the medical support staff.

The bisegmental absorption of the 750 μg dose gave initial conditions of $n_{10} = 9.5 \times 10^{-9}$ mol and $n_{20} = 19.3 \times 10^{-9}$ mol (a total of 28.8×10^{-9} mol) (Wang et al., 2001). We simulated wild-type GCSF with this initial dose. We then simulated both SD/01 and an SD/01-like ligand with 5-fold lower endosomal affinity than normal (possibly a PEG-modified histidine mutant of GCSF) with much lower hypothetical doses, $n_{10} = 2.5 \times 10^{-9}$ mol and $n_{20} = 2.5 \times 10^{-9}$ mol. This total available dose is only about 17% of that available from the 750 μg dose for wild-type GCSF.

The results for these three simulations are given in Fig. 9. Figure 9A shows a rapid and large increase in the wild-type concentration, but the ligand is then completely consumed in less than 2 days. By contrast, the maximum peak of SD/01 is lower but the ligand is sustained for about 6 days. The SD/01-like ligand with reduced endosomal affinity is not fully depleted during the time course. The impact on neutrophil counts is shown in Fig. 9B. The counts return to baseline after about 5 days for wild type, and they return to baseline after about 8 days for SD/01. However, the counts are more than 6-fold higher than baseline for the SD/01 analog with reduced endosomal affinity at the end of the time course.

Discussion

We have described here a hierarchical model that integrates a cell-level mathematical model of GCSF/GCSFR trafficking with a traditional pharmacokinetic/pharmacodynamic model. We have made predictions on in vivo behavior based on the sensitivities of parameters representing physiological processes, including molecular and cellular parameters in the subset of equations representing the cell-level model.

The base value of the parameter for nonspecific clearance, η, was fitted by Wang et al. (2001) in a PK/PD model based upon clinical data. Incremental reduction of this parameter in simulations led to greater ligand sustenance and enhanced neutrophil counts over time. In the presence of nonspecific clearance, decreases in the endosomal affinity were predicted to result in small increases in ligand concentration, with neutrophil profiles extended by up to one day. Our model probably underpredicts the magnitude of this effect, because other clinical data show a much more significant contribution

of cell-mediated clearance in the presence of nonspecific clearance mechanisms, leading to significant nonlinear pharmacokinetics (Layton et al., 1989; Morstyn et al., 1998). These nonlinearities are not seen at the extremes of high GCSF dosage (when receptor-mediated clearance would be saturated) or severe neutropenia (when the number of cells participating in receptor-mediated clearance would be very low) (Layton et al., 1989; Morstyn et al., 1998). Any additional weight on the receptor-mediated clearance pathway would only lend more credence to our conjecture that molecular and cellular parameters can significantly impact the potency of therapeutic proteins such as hematopoietic cytokines.

Many of the simulations focus on in vivo behavior in the absence of nonspecific clearance. SD/01, a GCSF analog with a 20-kDa PEG moiety at the N terminus, is essentially depleted by only specific cell-mediated clearance (Johnston et al., 2000). Interestingly, in the absence of these nonspecific clearance mechanisms, it has been suggested that SD/01 is self-regulating in vivo (Johnston et al., 2000). Part of this regulation is probably caused by the negative feedback loop depicted in Fig. 3. As neutrophil counts increase, the drug is then depleted to a greater extent, which in turn attenuates the increase in neutrophil production. As our model suggests, we further propose that this regulation can be tuned by also altering the molecular-level properties of the drug that impact cellular trafficking.

For example, SD/01 has a 3-fold lower affinity for GCSFR than wild-type GCSF. This slight reduction in extracellular binding affinity increases ligand concentration over time while maintaining neutrophil counts over a longer period of time compared with a hypothetical SD/01-like ligand with wild-type binding affinity (Fig. 6, A and B). The proposed self-regulation could be further improved by reducing the endosomal affinity of SD/01 (Fig. 8). We have rationally designed GCSF mutants (D110H and D113H) whose receptor-binding properties are more pH-sensitive than wild type. These mutants bind with lower affinities than wild type at endosomal pH and are therefore recycled to a much greater extent. If the effects of PEG-conjugation were superimposable upon the effects of one of these histidine mutants, the resulting PEG-conjugated analog (e.g., PEG-D110H or PEG-D113H) could have even more desirable therapeutic properties than either wild-type GCSF or SD/01 (Fig. 9). These could include lower dosing amounts, which could reduce toxicity and side effects, and less frequent dosing.

To the best of our knowledge, this is the first attempt to develop a hierarchical PK/PD model that provides a link between molecular parameters and physiological response. We believe that such a model could have great value in determining the parameters that play important roles in the pharmacokinetics and pharmacodynamics of a drug and may thus provide insights and design goals for developing next-generation therapeutics.

References

Delgado C, Francis GE, and Fisher D (1992) The uses and properties of PEG-linked proteins. *Crit Rev Ther Drug Carrier Syst* **9:**249–304.
Elsonbaty SS, Tsuchiya H, Watanabe M, Hochito K, Kunisada T, Shimosaka A, and

Matsuda I (1995a) Exogenous expression of human granulocyte colony-stimulating factor receptor in a B-lineage acute lymphoblastic leukemia cell line: a possible model for mixed lineage leukemia. *Leuk Res* **19:**249–256.

Elsonbaty SS, Watanabe M, Hochito K, Yamaguchi K, Matsuda I, and Tsuchiya H (1995b) Exogenously expressed granulocyte colony stimulating factor (G-CSF) receptor on K562 cells can transduce G-CSF triggered growth and differentiation signals. *Int J Hematol* **61:**61–68.

Fallon EM and Lauffenburger DA (2000) Computational model for effects of ligand/receptor binding properties on interleukin-2 trafficking dynamics and T cell proliferation response. *Biotechnol Prog* **16:**905–916.

Fallon EM, Liparoto SF, Lee KJ, Ciardelli TL, and Lauffenburger DA (2000) Increased endosomal sorting of ligand to recycling enhances potency of an interleukin-2 analog. *J Biol Chem* **275:**6790–6797.

French AR, Tadaki DK, Niyogi SK, and Lauffenburger DA (1995) Intracellular trafficking of epidermal growth factor family ligands is directly influenced by the pH sensitivity of the receptor/ligand interaction. *J Biol Chem* **270:**4334–4340.

Ghosh RN, Gelman DL, and Maxfield FR (1994) Quantification of low-density lipoprotein and transferrin endocytic sorting in HEP2 cells using confocal microscopy. *J Cell Sci* **107:**2177–2189.

Harris JM, Martin NE, and Modi M (2001) Pegylation: a novel process for modifying pharmacokinetics. *Clin Pharmacokinet* **40:**539–551.

Johnston E, Crawford J, Blackwell S, Bjurstrom T, Lockbaum P, Roskos L, Yang BB, Gardner S, Miller-Messana MA, Shoemaker D, et al. (2000) Randomized, dose-escalation study of SD/01 compared with daily filgrastim in patients receiving chemotherapy. *J Clin Oncol* **18:**2522–2528.

Khwaja A, Carver J, Jones HM, Paterson D, and Linch DC (1993) Expression and dynamic modulation of the human granulocyte colony stimulating factor receptor in immature and differentiated myeloid cells. *Br J Haematol* **85:**254–259.

Kuwabara T, Kobayashi S, and Sugiyama Y (1996) Kinetic analysis of receptor-mediated endocytosis of G-CSF derivative, nartograstim, in rat bone marrow cells. *Am J Physiol* **34:**E73–E84.

Lauffenburger DA and Linderman JJ (1993) *Receptors: Models for Binding, Trafficking and Signaling.* Oxford University Press, New York.

Layton JE, Hockman H, Sheridan WP, and Morstyn G (1989) Evidence for a novel in vivo control mechanism of granulopoiesis: mature cell-related control of a regulatory growth factor. *Blood* **74:**1303–1307.

Morikawa K, Morikawa S, Miyawaki T, Nagasaki M, Torii I, and Imai K (1996) Constitutive expression of granulocyte colony-stimulating factor receptor on a human B-lymphoblastoid cell line. *Br J Haematol* **94:**250–257.

Morstyn G, Dexter TM, and Foote M (1998) *Filgrastim (r-metHuG-CSF) in Clinical Practice,* Marcel Dekker, Inc., New York.

Morstyn G, Foote MA, Walker T, and Molineux G (2001) Filgrastim (r-metHuG-CSF) in the 21st century: SD/01. *Acta Haematol* **105:**151–155.

Sarkar CA (2002) *Cytokine Engineering through Ligand/Receptor Dynamics: a Study on Granulocyte Colony-Stimulating Factor.* Ph.D. Thesis, Massachusetts Institute of Technology, Cambridge, MA.

Sarkar CA, Lowenhaupt K, Horan T, Boone TC, Tidor B, and Lauffenburger DA (2002) Rational cytokine design for increased lifetime and enhanced potency using pH-activated 'histidine switching'. *Nat Biotechnol* **20:**908–913.

Wang B, Ludden TM, Cheung EN, Schwab GG, and Roskos LK (2001) Population pharmacokinetic-pharmacodynamic modeling of Filgrastim (r-metHuG-CSF) in healthy volunteers. *J Pharmacokinet Pharmacodyn* **28:**321–342.

Address correspondence to: Douglas A. Lauffenburger, Massachusetts Institute of Technology, Room 56–341, Cambridge, Massachusetts 02139-4307. E-mail: lauffen@mit.edu